ACS OMEGA

Open Access

http://pubs.acs.org/journal/acsodf

Article

Heterogeneous Transformation of Ginsenoside Rb1 with Ethanol Using Heteropolyacid-Loaded Mesoporous Silica and Identification by HPLC-MS

Mengya Zhao, Lu Tian, Yusheng Xiao, Yanyan Chang, Yujiang Zhou, Shuying Liu, Huanxi Zhao,* and Yang Xiu*

Cite This: *ACS Omega* 2023, 8, 43285−43294

Read Online

ACCESS | Metrics & More | Article Recommendations | Supporting Information

ABSTRACT: Rare ginsenosides with major pharmacological effects are barely present in natural ginseng and are required to be obtained by transformation. In the current study, ginsenoside Rb1 was chemically transformed with the involvement of ethanol molecules to prepare rare ginsenosides using the synthesized heterogeneous catalyst 12-HPW@MeSi. A total of 16 transformation products were obtained and identified using high-performance liquid chromatography coupled with multistage tandem mass spectrometry and high-resolution mass spectrometry. Ethanol molecules were involved in the production of 6 transformation products by adding to the C-20(21), C-20(22), or C-24(25) double bonds on the aglycone to produce ethoxyl groups at the C-25 and C-20 positions. Transformation pathways of ginsenoside Rb1 are summarized, which involve deglycosylation, elimination, cycloaddition, epimerization, and addition reactions. In addition, 12-HPW@MeSi was recyclable through a simple centrifugation, maintaining an 85.1% conversion rate of Rb1 after 3 cycles. This work opens up an efficient and recycled process for the preparation of rare ginsenosides with the involvement of organic molecules.

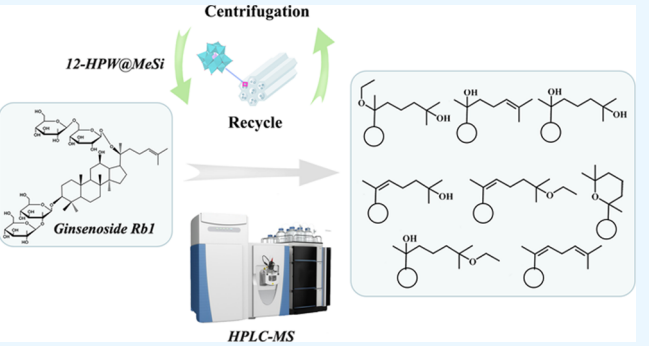

1. INTRODUCTION

Ginsenosides are regarded as the major active components of ginseng and are well characterized for their pharmacological effects.[1−3] In ginseng, they are primarily of the dammarane type and have a dammarane backbone coupled with glycosyl substituents. Based on the number and position of the hydroxyl group linkage, ginsenosides are generally classified into protopanaxadiol (PPD) and protopanaxatriol (PPT) types.[4−6] At present, more than 100 ginsenosides have been isolated and identified, of which the major ones such as Rb1, Rb2, Rg1, Rc, and Re have been determined to account for over 80% of the total content of ginsenosides, while the other ginsenosides such as Rg3, Rg5, and Rk1 are known as rare ginsenosides due to their low content in ginseng.[1,7] Studies have shown that rare ginsenosides have more remarkable pharmaceutical activities and that they differ from the major ginsenosides in terms of glycosyl substituents and side-chain structures.[8] Therefore, much effort has been focused on the chemical transformation and biotransformation of major ginsenosides into rare ginsenosides by modifying their glycosyl substituents and side chains.[9,10]

The conventional chemical transformation of ginsenosides mainly uses liquid acids for homogeneous catalytic transformation, which benefits from high efficiency and low cost, but suffers from difficult separation of product and catalyst.[11,12] Heteropolyacids (HPAs) are a kind of inorganic solid acid and have been used to catalyze many types of reactions owing to their strong proton acidity, adjustable structure, and multiphase catalytic ability.[13−15] They also provide a new pathway for the chemical transformation of ginsenosides. However, their good solubility in polar media renders them not conducive to separation and recycling. And, as with the conventional liquid acids, homogeneous catalysis is disadvantageous for the transformation of ginsenosides in water.[16] To achieve a heterogeneous transformation environment, HPAs can be loaded with porous solid supports to maintain their original solid acidity.[17−19] The silica supports are particularly favorable due to their large specific surface area, excellent thermal stability, and chemical inertness.[20−22] Studies have shown that examples of success are frequently associated with

Received: September 20, 2023
Revised: October 16, 2023
Accepted: October 17, 2023
Published: October 31, 2023

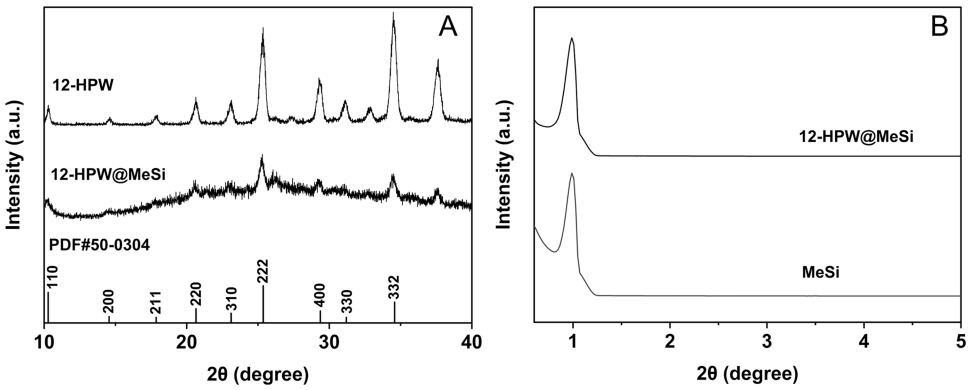

Figure 1. Powder X-ray diffraction patterns of 12-HPW and 12-HPW@MeSi over the 2θ range of 10−40° (A) and MeSi and 12-HPW@MeSi over the 2θ range of 0.6−5° (B).

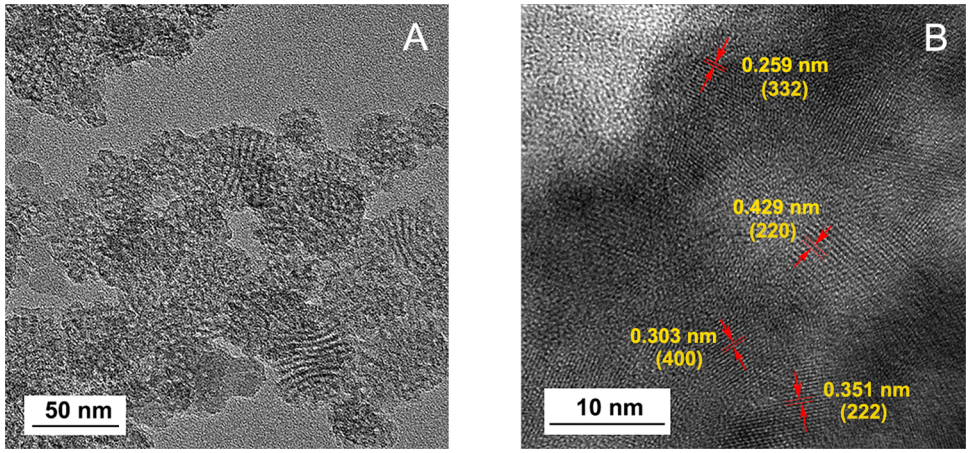

Figure 2. TEM image of MeSi (A) and HRTEM image of 12-HPW@MeSi (B).

the use of silica supports. For example, Yang et al. synthesized the mesoporous silica-included HPAs material as a solid catalyst for the alkylation of phenol with cyclohexene, which maintained stable activity over six cycles.[23] However, the application of loaded HPAs in the heterogeneous transformation of ginsenosides has not been reported. In addition, the reported preparation of rare ginsenosides usually employs the degradation of the major ginsenosides within themselves.[24] For example, Bai et al. reported the use of *Lactobacillus plantarum* to remove the sugar group at the C-20 position of ginsenoside Re and obtain ginsenoside Rg6 and F4.[25] Theoretically, the dammarane-type ginsenosides contain a double bond functional group on the olefinic chain, which provides ample opportunity to use electrophilic addition reactions to modify the structure and thus produce rare ginsenosides with novel structures. The involvement of small organic molecules in the transformation of ginsenosides to prepare rare ginsenosides, however, has not been extensively investigated.

High-performance liquid chromatography−mass spectrometry (HPLC-MS) has evolved into one of the main research tools for the structural identification and quantitative analysis of natural products.[26−28] It combines component separation with quantitative analysis or qualitative identification and provides an effective means of analyzing complex samples. Among them, HPLC coupled with high-resolution MS (HPLC-HRMS) enables highly sensitive and accurate sample detection,[29] while HPLC coupled with multistage tandem MS ($HPLC\text{-}MS^n$) provides information on characteristic fragment ions which, combined with neutral loss and cleavage patterns, allow for rapid determination of structural information on compounds.[30]

In this study, the composite solid acid catalyst 12-HPW@MeSi was synthesized through the assembly of 12-phosphotungstic acid (12-HPW) and mesoporous silica (MeSi) and used for the heterogeneous transformation of ginsenoside Rb1 in aqueous ethanol solution. Sixteen rare ginsenosides were obtained, and their structures and transformation pathways were extensively investigated by $HPLC\text{-}MS^n$ and HRMS. Ethanol molecules were found to participate in the transformation, producing ethoxylated ginsenosides. Meanwhile, 12-HPW@MeSi was tested for its reusability as a heterogeneous catalyst in ginsenoside transformation.

2. RESULTS AND DISCUSSION

2.1. Characterization of 12-HPW@MeSi. Characterization of MeSi and 12-HPW@MeSi was carried out by powder X-ray diffraction (XRD). The wide-angle XRD patterns of 12-HPW and 12-HPW@MeSi are shown in Figure 1A. The 12-HPW used exhibits distinctive diffraction peaks that are well in line with hydrogen tungsten phosphate hydrate (PDF #50-0304). The peak intensity is greatly reduced after 12-HPW was immobilized on MeSi, although several diffraction peaks on the primary lattice planes of (222), (332), and (220) are retained. This indicates that 12-HPW has been successfully loaded onto MeSi and that the characteristic

https://doi.org/10.1021/acsomega.3c07214
ACS Omega 2023, 8, 43285−43294

Scheme 1. Chemical Transformation Pathway of Ginsenoside Rb1 Catalyzed by 12-HPW@MeSi

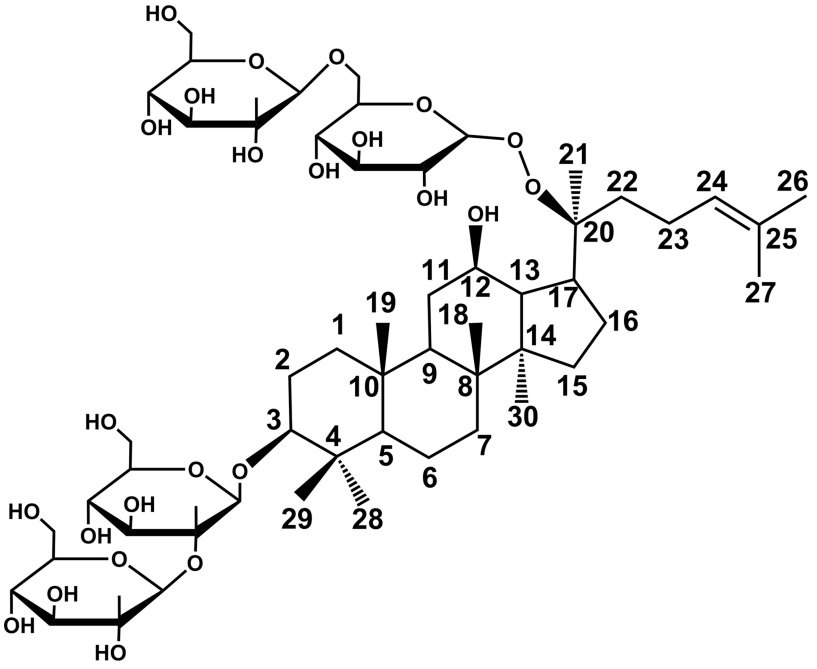

Keggin-type structure is retained. The observed decrease in the intensity of the diffraction peaks after immobilization is due to the dispersion of 12-HPW inside the channels of MeSi. As shown in Figure 1B, a diffraction peak can be observed at 0.9° in the small-angle XRD pattern of MeSi, indicating the presence of nonuniform but large mesopores in the synthesized MeSi. This peak is maintained for 12-HPW@MeSi, indicating that the introduction of 12-HPW did not affect the mesoporous structure of the MeSi support, which facilitated the contact and reaction of ginsenosides with loaded 12-HPW.

Figure 2 depicts the transmission electron microscopy (TEM) and high-resolution transmission electron microscopy (HRTEM) images of the synthesized MeSi and 12-HPW@MeSi. Figure 2A clearly shows the apertures and ordered arrays of hexagonal channels of MeSi, demonstrating the successful synthesis of mesoporous silica that can be used to accommodate 12-HPW. Figure 2B shows several apparently aligned lattices in 12-HPW@MeSi. By measuring the lattice spacing, matching crystal planes (222), (332), (400), and (220) were discovered. These planes are compatible with the XRD results and indicate that the 12-HPW species are uniformly embedded throughout the MeSi supports.

2.2. Structural Characterization of Ginsenoside Rb1 Transformation Products with Ethanol by HPLC-MS^n/HRMS. The synthesized 12-HPW@MeSi was used for the chemical transform ginsenoside Rb1 in 30% ethanol aqueous solution over the course of 8 h at 80 °C. The structural information on ginsenoside Rb1 is shown in Scheme 1. There are 16 products with distinct retention times, designated compounds **1**−**16**, as seen in Figure 3 of the total ion chromatogram (TIC). According to this result, the heterogeneous catalyst of 12-HPW@MeSi is able to transform ginsenoside Rb1 into rare ginsenosides. Using an established multistage tandem MS and high-resolution MS method, a thorough investigation of the structures of the transformation products was carried out.

The relative molecular weights of compounds **3** and **5** were calculated from their $[M + HCOO]^-$ and $[M - H]^-$ ions to be

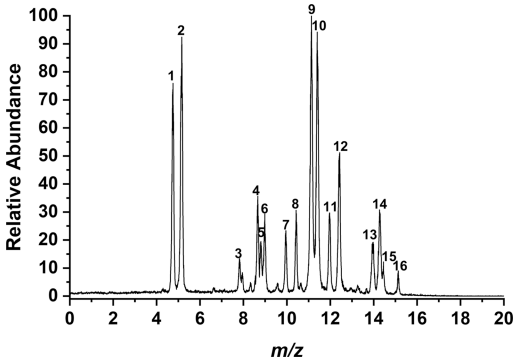

Figure 3. TIC of the transformation products of ginsenoside Rb1 with ethanol.

830.54. The fragment ions in their tandem mass spectra were identical, indicating that they were a pair of isomers. The tandem MS spectrum of compound **3** was used as an example to identify their structures, as shown in Figure 4A. The ion at m/z 667.48 is the fragment ion that removes one glucose substituent from the parent ion at m/z 829.54. The ion at m/z 621.44 has a mass difference of 46.04 Da with it, which corresponds to the molecular weight of ethanol (C_2H_5OH), indicating that compound **3** contains one ethoxyl group. The ion at m/z 459.38 is the fragment ion of the parent ion that removes two glucose substituents and one ethanol molecule. The ion at m/z 401.34 has a mass difference of −58.04 Da with it, corresponding to the tertiary alcohol structure formed by the addition of one water molecule to the C-24(C25) double bond. This indicates that compound **3** has undergone a hydration reaction. The difference between the aglycone ion of compound **3** at m/z 505.42 and that of PPD at 459.38 Da is 46.04 Da. The hydration reaction leads to an increase in the aglycone ion by 18.01 Da, while the remaining difference of 28.03 Da can only result from the substitution of the hydroxyl group at the C-20 position by the ethoxyl group. It can be concluded that compound **3** is the product of Rb1 dissociating

https://doi.org/10.1021/acsomega.3c07214
ACS Omega 2023, 8, 43285−43294

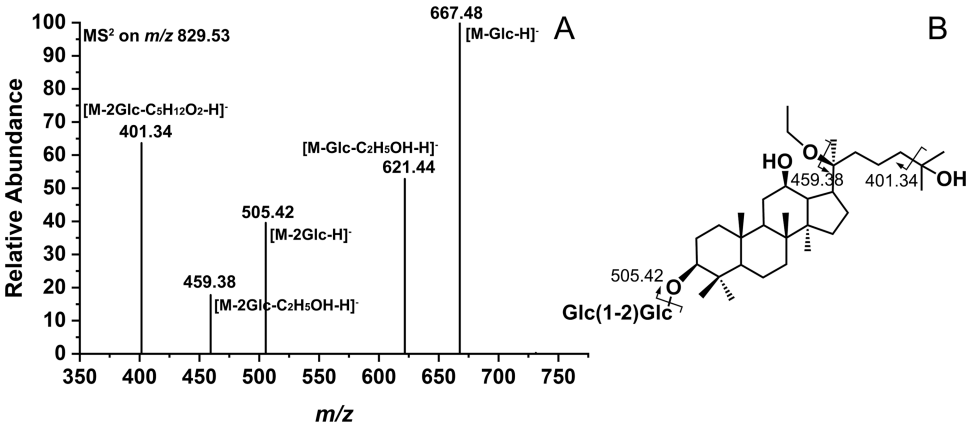

Figure 4. MS^2 spectrum of the $[M - H]^-$ ion at m/z 829.53 from the ginsenoside 20(S)-OC_2H_5-25-OH-Rg3 (A). Fragmentation pathways of ginsenoside 20(S)-OC_2H_5-25-OH-Rg3 (B).

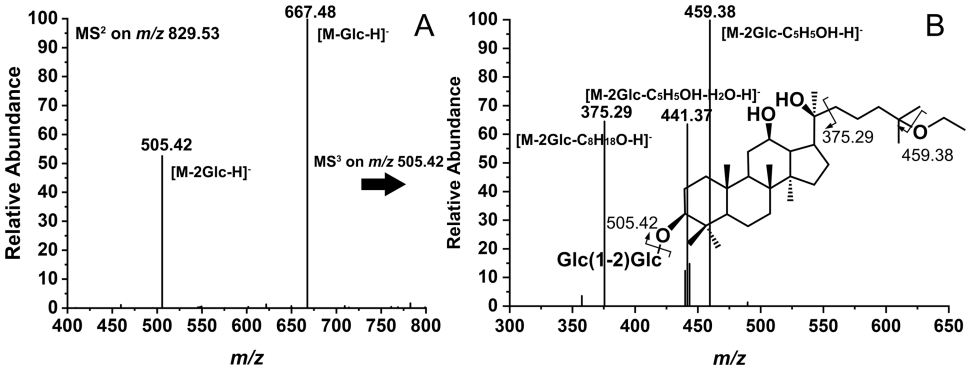

Figure 5. MS^2 spectrum of the $[M - H]^-$ ion at m/z 829.53 of ginsenoside 20(S)-25-OC_2H_5-Rg3 (A). Fragmentation pathways and MS^3 spectrum of the $[M\text{-}Glc\text{-}H]^-$ ion at m/z 505.42 of ginsenoside 20(S)-25-OC_2H_5-Rg3 (B).

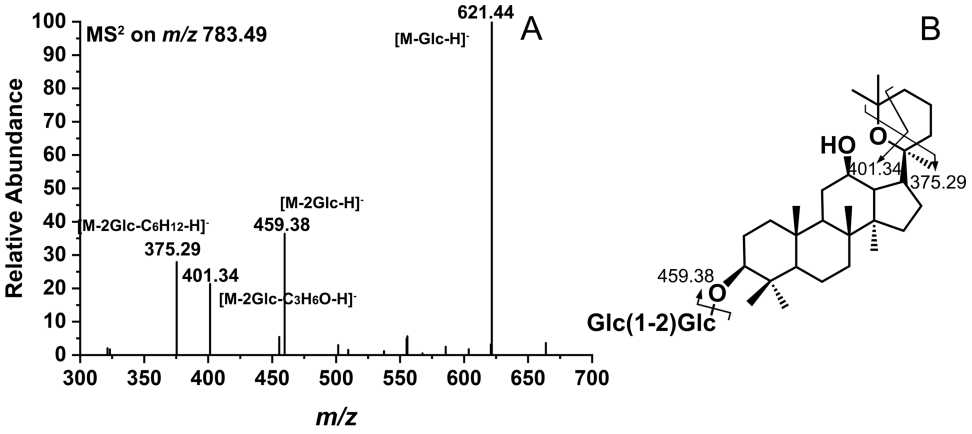

Figure 6. MS^2 spectrum of the $[M - H]^-$ ion at m/z 783.49 from the ginsenoside (20S, 25)-epoxy-Rg3 (A). Fragmentation pathways of ginsenoside (20S, 25)-epoxy-Rg3 (B).

the glucose substituent at the C-20 position, generating an ethoxyl group at the C-20 position, and undergoing a hydration reaction at the C-24(C25) double bond. Therefore, compounds **3** and **5** are classified as 20(S)-OC_2H_5-25-OH-Rg3 (Figure 4B) and 20(R)-OC_2H_5-25-OH-Rg3 (Figure S1), respectively. There are no intact aglycone ions in the tandem MS spectrum but obvious fragment ions that remove ethoxyl groups. This suggests that the ethoxy group at the C-20 position is more easily dissociated than the glycosidic bond at the C-3 position.

Compounds **7** and **8** are epimers with a relative molecular weight of 830.54. Their structures were analyzed by taking the tandem MS spectrum of compound **7** as an example. As shown in the MS^2 spectrum in Figure 5A, the fragment ions at m/z 667.48 and m/z 505.42 are generated by removing one and two glucose substituents from the parent ion at m/z 829.53, respectively. The latter ion is the aglycone ion of compound **7** and is further fragmented by MS^3. The resulting MS^3 spectrum is shown in Figure 5B. The ion at m/z 459.38 differs from the aglycone ion at m/z 505.42 by 46.04 Da, corresponding to one ethanol molecule, indicating the presence of at least one ethoxy

https://doi.org/10.1021/acsomega.3c07214
ACS Omega 2023, 8, 43285−43294

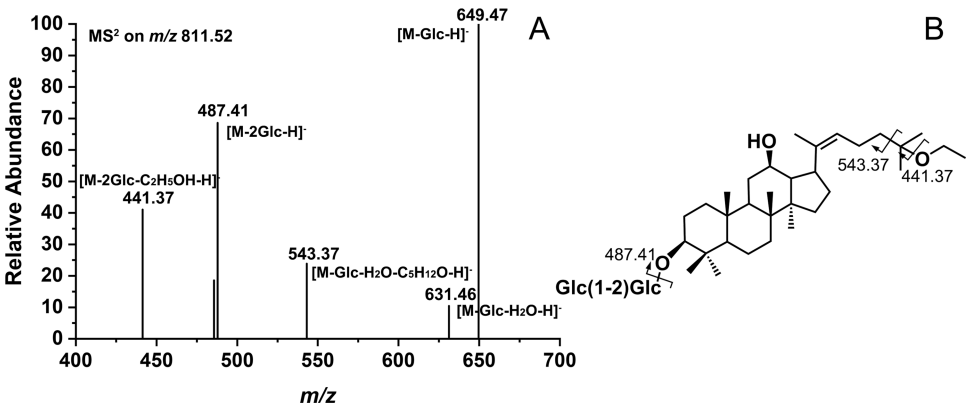

Figure 7. MS^2 spectrum of the $[M - H]^-$ ion at m/z 811.52 from the ginsenoside 25-OC_2H_5-Rg5 (A). Fragmentation pathways of ginsenoside 25-OC_2H_5-Rg5 (B).

group in the structure of compound **7**. The characteristic ion at m/z 375.29 results from the cleavage of the single bond at the C-20(22) double bond of PPD-type ginsenosides. Its presence indicates that the hydroxyl group at the C-20 position is not substituted by the ethoxyl group, and therefore the ethanol molecule should add to the C-24(25) double bond. Based on the above analysis, compounds **7** and **8** are identified as 20(S)-25-OC_2H_5-Rg3 and 20(R)-25-OC_2H_5-Rg3 (Figure S2), respectively.

Compounds **9** and **10** are isomers with the same relative molecular weight of 784.50. The tandem MS spectrum of compound **9** is shown in Figure 6A. The product ions at m/z 621.44 and m/z 459.38 indicate the presence of two glucose substituents in compound **9** and the latter is the aglycone ion. The neutral losses between the aglycone ion at m/z 459.38 and the product ions at m/z 401.34 and m/z 375.29 are 58.04 and 84.09 Da, respectively. The former neutral loss of 58.04 Da corresponds to the isopropanol group at the C-25 position as mentioned above. The latter neutral loss of 84.09 Da corresponds to the C_6H_{12} molecule, representing the olefin chain at the C-20 position of PPD. From the coexistence of the two neutral losses, it can be inferred that compound **9** is generated by the cycloaddition of the C-24(25) double bond and the hydroxyl group at the C-20 position. Therefore, compounds **9** and **10** were identified as (20S, 25)-epoxy-Rg3 (Figure 6B) and (20R, 25)-epoxy-Rg3 (Figure S3), respectively.

Compounds **13** and **14** are a pair of isomers with the same relative molecular weight of 812.53 Da. As shown in Figure 7A, the aglycone ion of compound **13** at m/z 487.41 is generated by removing two glucose substituents from the $[M - H]^-$ ion at m/z 811.52. It has a mass difference of 46.04 Da with the product ion at m/z 441.37, suggesting the presence of one ethoxyl group. The neutral loss of 88.09 Da between the product ions at m/z 631.46 and m/z 543.37 corresponds to the $C_5H_{12}O$ molecule, which indicates the presence of the 2-ethoxypropane group at the C-25 position originating from the addition of an ethanol molecule at the C-24(25) double bond. In addition, the mass difference between the ion at m/z 487.41 and the aglycone ion of PPD at m/z 459.38 is 28.03 Da. The mass difference generated by adding one ethanol molecule at the C-24(25) double bond is 46.04 Da, indicating that a hydration reaction also occurred at the C-20 position of the aglycone to counteract the additional 18.01 Da. Compounds **13** and **14** are therefore supposed to be produced by the hydrolysis of the disaccharide substituents of Rb1, the dehydration at the C-20 position, and the addition of an ethanol molecule at the C-24(25) double bond. And they are identified as the Δ 20(21) and Δ 20(22) isomers of 25-OC_2H_5-Rk1 (Figure 7B) and 25-OC_2H_5-Rg5 (Figure S4), respectively.

The tandem MS spectra of compounds **1**, **2**, **4**, and **6** (Figures S5−S8) were analyzed in the same manner. Compounds **1**, **2**, **4**, and **6** were identified as 20(S)-25-OH-Rg3, 20(R)-25-OH-Rg3, 25-OH-Rk1, and 25-OH-Rg5, respectively, on the basis of the mass difference with PPD in the aglycone ion and the presence of the characteristic neutral loss of 58.04 Da. By comparing the relative retention time and the tandem MS spectra with those of authentic standards, compounds **9**, **10**, **15**, and **16** were determined to be 20(S)-Rg3, 20(R)-Rg3, Rk1, and Rg5, respectively, and their structures and tandem MS spectral information are shown in Figures S9−S12. The characteristic fragment ions of all of the transformation products are summarized in Table 1.

2.3. Pathways and Mechanisms of the Chemical Transformation of Rb1 with Ethanol. In summary, a total of 16 ginsenosides were obtained by the chemical transformation of ginsenoside Rb1 in aqueous ethanol solution with the participation of 12-HPW@MeSi. The observed transformation pathways involve deglycosylation, elimination, cycloaddition, epimerization, and addition reactions, as shown in Scheme 2.

The reactant Rb1 contains two disaccharide substituents that are attached to the C-3 and C-20 positions. The C-20 position is a quaternary carbon, which exhibits a higher reactivity compared to the tertiary carbon at the C-3 position. In other words, the secondary carbenium ion at the C-3 position is less stable than the tertiary carbenium ion at the C-20 position produced by the cleavage of the glycosidic bond.[31] In the acidic environment created by 12-HPW@MeSi, the disaccharide substituent at the C-20 position is more prone to hydrolysis than its counterpart at C-3, and the major products, 20(S)-Rg3 and 20(R)-Rg3, are formed. Even after an 8 h chemical transformation, the disaccharide substituent at the C-3 position remains relatively stable. The formed Rg3 epimers serve as intermediate products for subsequent reactions that generate epimer products from different configurations of the chiral carbon atom at the C-20 position.

The hydroxyl group at the C-20 position in 20(S/R)-Rg3 can easily undergo protonation in the presence of a protonic acid catalyst, weakening the C−O bond, which in turn undergoes monomolecular elimination reactions to produce

https://doi.org/10.1021/acsomega.3c07214
ACS Omega 2023, 8, 43285−43294

Table 1. Information on the Identified Chemical Transformation Products of Ginsenoside Rb1 with Ethanol

peak	identification	molecular weight	molecular formula	$[M-H]^-$ measured value	fragment ions
1	20(S)-25-OH-Rg3	802.51	$C_{42}H_{74}O_{14}$	801.50	639.45[M-Glc-H]$^-$, 477.39[M-2Glc-H]$^-$
2	20(R)-25-OH-Rg3	802.51	$C_{42}H_{74}O_{14}$	801.50	639.45[M-Glc-H]$^-$, 477.39[M-2Glc-H]$^-$
3	20(S)-OC_2H_5-25-OH-Rg3	830.54	$C_{44}H_{78}O_{14}$	829.53	667.48[M-Glc-H]$^-$, 621.44[M-Glc-C_2H_5OH-H]$^-$, 505.42[M-2Glc-H]$^-$, 459.38[M-2Glc-C_2H_5OH-H]$^-$, 401.34[M-2Glc-$C_5H_{12}O_2$-H]$^-$
4	25-OH-Rk1	784.50	$C_{42}H_{72}O_{13}$	783.49	621.44[M-Glc-H]$^-$, 459.38[M-2Glc-H]$^-$, 401.34[M-2Glc-C_3H_6O-H]$^-$
5	20(R)-OC_2H_5-25-OH-Rg3	830.54	$C_{44}H_{78}O_{14}$	829.53	667.48[M-Glc-H]$^-$, 621.44[M-Glc-C_2H_5OH-H]$^-$, 505.42[M-2Glc-H]$^-$, 459.38[M-2Glc-C_2H_5OH-H]$^-$, 401.34[M-2Glc-$C_5H_{12}O_2$-H]$^-$
6	25-OH-Rg5	784.50	$C_{42}H_{72}O_{13}$	783.49	621.44[M-Glc-H]$^-$, 459.38[M-2Glc-H]$^-$, 401.34[M-2Glc-C_3H_6O-H]$^-$
7	20(S)-25-OC_2H_5-Rg3	830.54	$C_{44}H_{78}O_{14}$	829.53	667.48[M-Glc-H]$^-$, 505.42[M-2Glc-H]$^-$, 459.38[M-2Glc-C_2H_5OH-H]$^-$, 441.37[M-2Glc-C_2H_5OH-H_2O-H]$^-$, 375.29[M-2Glc-$C_8H_{18}O$-H]$^-$
8	20(R)-25-OC_2H_5-Rg3	830.54	$C_{44}H_{78}O_{14}$	829.53	667.48[M-Glc-H]$^-$, 505.42[M-2Glc-H]$^-$, 459.38[M-2Glc-C_2H_5OH-H]$^-$, 441.37[M-2Glc-C_2H_5OH-H_2O-H]$^-$, 375.29[M-2Glc-$C_8H_{18}O$-H]$^-$
9	20(S)-Rg3	784.50	$C_{42}H_{72}O_{13}$	783.49	621.44[M-Glc-H]$^-$, 459.38[M-2Glc-H]$^-$, 375.29[M-2Glc-C_6H_{12}-H]$^-$
10	20(R)-Rg3	784.50	$C_{42}H_{72}O_{13}$	783.49	621.44[M-Glc-H]$^-$, 459.38[M-2Glc-H]$^-$, 375.29[M-2Glc-C_6H_{12}-H]$^-$
11	20(S,25)-epoxy-Rg3	784.50	$C_{42}H_{72}O_{13}$	783.49	621.44[M-Glc-H]$^-$, 459.38[M-2Glc-H]$^-$, 401.34[M-2Glc-C_3H_6O-H]$^-$, 375.29[M-2Glc-C_6H_{12}-H]$^-$
12	20(R,25)-epoxy-Rg3	784.50	$C_{42}H_{72}O_{13}$	783.49	621.44[M-Glc-H]$^-$, 459.38[M-2Glc-H]$^-$, 401.34[M-2Glc-C_3H_6O-H]$^-$, 375.29[M-2Glc-C_6H_{12}-H]$^-$
13	25-OC_2H_5-Rk1	812.52	$C_{44}H_{76}O_{13}$	811.52	649.47[M-Glc-H]$^-$, 631.46[M-Glc-H_2O-H]$^-$, 487.41[M-2Glc-H]$^-$, 441.37[M-2Glc-C_2H_5OH-H]$^-$
14	25-OC_2H_5-Rg5	812.52	$C_{44}H_{76}O_{13}$	811.52	649.47[M-Glc-H]$^-$, 631.46[M-Glc-H_2O-H]$^-$, 487.41[M-2Glc-H]$^-$, 441.37[M-2Glc-C_2H_5OH-H]$^-$
15	Rk1	766.49	$C_{42}H_{70}O_{12}$	765.48	603.43[M-Glc-H]$^-$, 441.37[M-2Glc-H]$^-$
16	Rg5	766.49	$C_{42}H_{70}O_{12}$	765.48	603.43[M-Glc-H]$^-$, 441.37[M-2Glc-H]$^-$

alkenes.[32] The carbenium ion intermediates are also formed during this reaction, which follows the E1 reaction mechanism, while the rate of the reaction is only related to the concentration of the reactants. Since the high concentration of intermediate 20(S/R)-Rg3 at the initial stage of the Rb1 conversion reaction, it is more conducive to the elimination reaction of hydroxyl at the C-20 position to generate products Rk1 and Rg5. This result follows Zaitsev's rule, that is, it is easier to generate olefins with more substituents.[33]

In an acid environment, the double bond at the C-24(25) double bond is susceptible to addition reactions with electrophilic reagents.[34] This results in transformation products with the electrophilic group added specifically at the C-25 position. During the ethanol-involved chemical transformation of Rb1, both water and ethanol molecules can act as electrophilic reagents to react with the double bond, leading to the formation of the isopropanol and 2-ethoxypropane groups at the C-25 position, respectively. The mechanism for this process follows Markovnikov's rule; i.e., the electrophilic group is added at the C-25 position, which can be explained theoretically in terms of the stability of the carbenium ion intermediate. The eight products 20(S/R)-25-OH-Rg3, 20(S/R)-25-OC_2H_5-Rg3, 25-OH-Rg5, 25-OH-Rk1, 25-OC_2H_5-Rk1, and 25-OC_2H_5-Rg5 were generated through this transformation pathway. In addition, the newly formed double bonds at the C-20(21) and C-20(22) double bonds in Rk1 and Rg5 are also able to undergo addition reactions with water and ethanol molecules, which is similar to the previous reaction process involving the double bond at the C-24(25) double bond. In this instance, hydroxyl and ethoxyl groups are added at the C-20 position, resulting in the formation of products such as 20(S/R)-OC_2H_5-25-OH-Rg3. Remarkably, the hydroxyl group located at the C-20 position can also act as an electrophilic group, participating in the addition reaction with the double bond at the C-24(25) double bond. The products of 20(S/R,25)-epoxy-Rg3 with an oxygenated six-membered ring are obtained from this cycloaddition pathway.

In addition, the addition of the double bond is mutually reversible with the elimination of the hydroxyl and ethoxyl groups under acidic conditions. For example, as shown in Scheme 2, 25-OC_2H_5-Rk1 and 25-OC_2H_5-Rg5 can be formed by adding the ethoxyl group at the C-25 position of Rk1 and Rg5, whereas Rk1 and Rg5 can be reversibly formed by the elimination of an ethanol molecule at the C-24(25) double bond of 25-OC_2H_5-Rk1 and 25-OC_2H_5-Rg5, demonstrating that there is a dynamic chemical equilibrium between the addition products of olefins with water and ethanol molecules.

2.4. Optimization for the Chemical Transformation of Ginsenoside Rb1 with Ethanol. The effects of the transformation time, temperature, and ethanol concentration on the transformation of ginsenoside Rb1 were investigated.

As shown in Figure 8A, after 1 h of transformation in 30% ethanol aqueous solution, the unreacted Rb1 and main products of 20(S/R)-Rg3, Rk1, Rg5, 25-OC_2H_5-Rk1, and 25-OC_2H_5-Rg5 can be observed. 20(S/R)-Rg3 predominates among the products since it requires only one step of deglycosylation from Rb1 for its generation. The high peak areas of Rk1 and Rg5 indicate that the hydroxyl group at C-20 is prone to an elimination reaction. These main products acted as important intermediates and were further transformed into the other 10 products, as shown in Figure 8B,8C. By comparing the peak areas of the transformation products at different times, it can be seen that the transformation of Rb1 is

https://doi.org/10.1021/acsomega.3c07214
ACS Omega 2023, 8, 43285−43294

Scheme 2. Chemical Transformation Pathways of Ginsenoside Rb1 with Ethanol

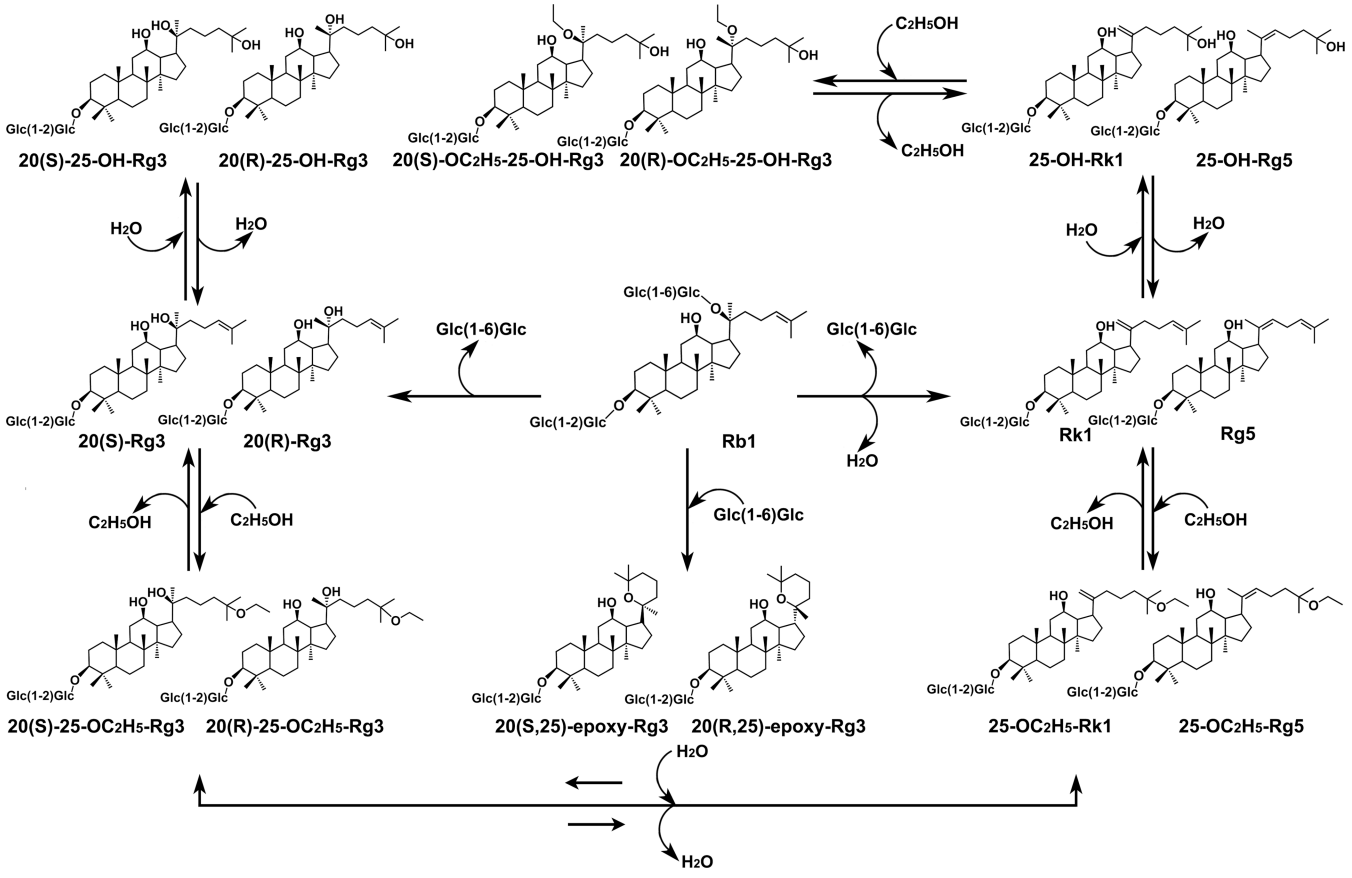

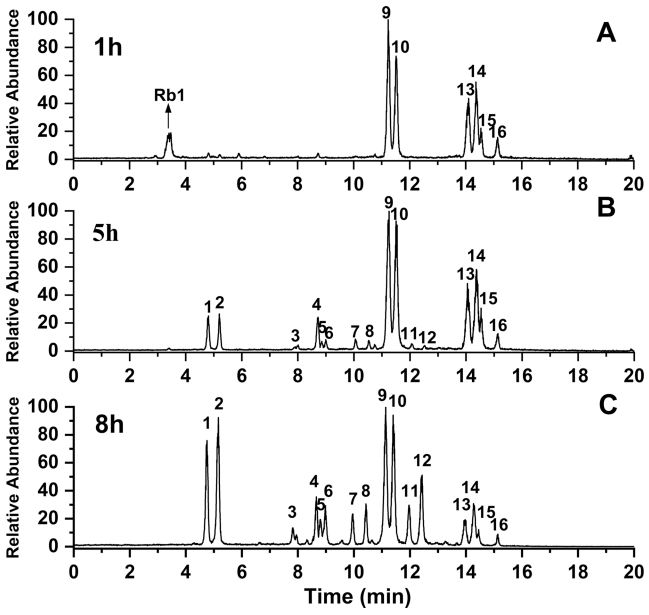

Figure 8. TIC of the transformation products of ginsenoside Rb1 with ethanol at 1 h (A), 5 h (B), and 8 h (C).

initially a deglycosylation reaction, followed by further elimination and addition reactions.

Temperature has a significant effect on the transformation of Rb1, the results of which are shown in Figure 9A. The six main products, including 20(S/R)-Rg3, Rk1, Rg5, 25-OC_2H_5-Rk1, and 25-OC_2H_5-Rg5, are completely dominating after 5 h of transformation at 40 °C. This further confirms that the deglycosylation at the C-20 position, addition to the C-24(25) double bond, and elimination of the C-20 hydroxyl group occur with relative ease. The peak areas of these six main products dramatically decrease with increasing temperature as a result of their continued transformation, while the other 10 products gradually appear. This indicates that the transformation of Rb1 is thermodynamically favorable and that higher temperatures can accelerate the transformation.

The ethanol concentration directly influences the formation of addition products of the C-24(25) double bond. Figure 9B illustrates that at an ethanol concentration of 30%, the water molecule adducts of 25-OH-Rk1, 25-OH-Rg5, and 20(S/R)-25-OH-Rg3 are clearly observed. When the ethanol concentration was increased to 50 and 70%, fewer water molecular adducts were obtained within the same reaction time, while a large number of ethanol molecular adducts were produced, such as the main products 25-OC_2H_5-Rk1 and 25-OC_2H_5-Rg5. This suggests that the water addition to the C-24(25) double bonds of Rk1 and Rg5 appears to react more readily than ethanol at a lower ethanol concentration, while the water molecule adducts are further inhibited as the proportion of ethanol is increased. This means that the ethanol concentration affects the formation of the addition products, and the addition of water and ethanol molecules at the C-24(25) double bond competes with each other.

2.5. Reusability of 12-HPW@MeSi. The synthesized 12-HPW@MeSi was recycled in the transformation of Rb1 with ethanol by simple centrifugation, washed with ethanol, and dried at 50 °C. The recycling of 12-HPW@MeSi is evaluated by the conversion rate of Rb1 and is carried out in 30% ethanol

https://doi.org/10.1021/acsomega.3c07214
ACS Omega 2023, 8, 43285−43294

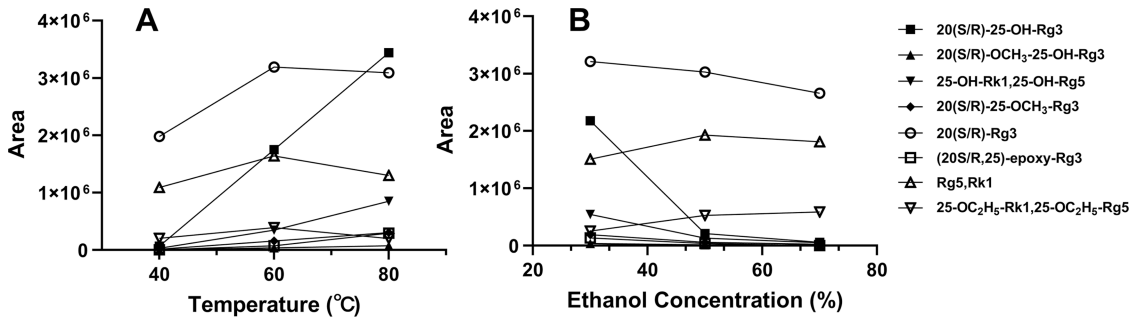

Figure 9. Peak areas of the transformation products of Rb1 with ethanol at varied ethanol concentration (A) and temperature (B).

aqueous solution at 80 °C for 5 h. The results are illustrated in Figure 10. It could be observed that the conversion rate of Rb1

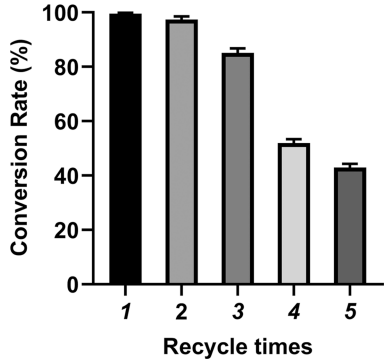

Figure 10. Conversion rate of Rb1 for different cycle times.

transformed by the fresh catalyst is up to ca. 100% and remained at 85.1% after three consecutive cycles. A clear downward trend after three cycles is then observed, which could be attributed to the degradation of the host MeSi framework and the release of the immobilized 12-HPW. In summary, 12-HPW@MeSi can be easily separated from the solution after the reaction by simple centrifugation and demonstrates a considerable degree of reusability, which is of great importance for practical applications.

3. CONCLUSIONS

12-HPW was successfully loaded in the mesoporous MeSi host, as characterized by TEM and XRD, resulting in the composite catalyst 12-HPW@MeSi. It was used for the heterogeneous chemical transformation of ginsenoside Rb1 with the involvement of ethanol molecules. A total of 16 transformation products were obtained. In particular, ethanol was involved in the production of 6 transformation products, which were formed by adding ethanol molecules to the C-20(22), C-20(21), and C-24(25) double bonds, generating ethoxyl groups at the C-20 and C-25 positions. The chemical transformation pathways of ginsenoside Rb1 include deglycosylation, elimination, cycloaddition, epimerization, and competitive addition between water and ethanol molecules, all of which are thermodynamically favored. Moreover, 12-HPW@MeSi could be recovered by simple centrifugation and recycled. It was able to maintain an 85.1% conversion rate of Rb1 after 3 cycles. The heterogeneous catalytic system combined with organic solvent molecules provides an efficient and recyclable strategy for the preparation of rare ginsenosides. In addition, the introduction of organic solvent molecules into the transformation reaction offers multiple possibilities to produce ginsenosides with novel structures.

4. EXPERIMENTAL SECTION

4.1. Chemicals and Materials. 12-HPW and ginsenoside Rb1 were acquired from Shanghai Yuanye Biological Technology Co., Ltd. (Shanghai, China). Hexadecyl trimethylammonium bromide (CTAB), tetraethyl orthosilicate (TEOS), and ammonium hydroxide bromide ($NH_3{\cdot}H_2O$) were purchased from Shanghai Macklin Biochemical Co., Ltd. HPLC-grade acetonitrile and ethanol were purchased from Tedia (Fairfield). HPLC-grade formic acid was acquired from Thermo Fisher (Waltham). Distilled water was prepared with a Milli-Q system (Millipore, Bedford). All chemicals were used as received without further purification.

4.2. Instrumentation and Conditions. XRD analyses were collected at ambient temperature on a TDM-10 X-ray diffractometer (Dandong Tongda Technology Co., Ltd., Liaoning, China), using Cu Kα radiation (Kα1 wavelength 1.5418 Å) at 40 kV and 30 mA, in the range from $0.6 \leq 2\theta \leq 5°$ and $5 \leq 2\theta \leq 40°$. HRTEM images were taken by a JEOL JEM-2100f operating at 200 kV.

Chromatographic separation was performed on an Ultimate 3000 system (Thermo Scientific, San Jose, CA) coupled with a Thermo Syncronis C18 column (100 × 2.1 mm, 1.7 μm). The column oven temperature was maintained at 35 °C, and the mobile phases A and B were water with 0.1% formic acid and acetonitrile, respectively. The separation of experimental samples was programmed with the following gradient elution: 25−25% (B, 0−3 min), 25−36% (B, 3−5 min), 36−48% (B, 5−8 min), 48−70% (B, 8−11 min), 70−90% (B, 11−17 min), and 90−25% (B, 17−20 min). The injection volume was 2 μL, and the flow rate was 0.2 mL/min.

Multistage tandem MS analysis was carried out on the LTQ-XL mass spectrometer (Thermo Scientific, San Jose, CA), while full-scan analysis and secondary tandem MS analysis were carried out on a Q-Exactive hybrid quadrupole-orbitrap mass spectrometer (Thermo Scientific, San Jose, CA), both equipped with an electrospray ionization source (ESI) operated in negative ion mode. The parameters of the ion source were set as follows: sheath gas, 35 arb units; auxiliary gas, 10 arb units; sweep gas, 1 arb unit; capillary voltage, −3200 V. The scan range was from m/z 100 to 1500 for full-scan mode and from m/z 200 to 1000 for tandem mode.

4.3. Sample Preparation. *4.3.1. Preparation of MeSi.* 561 mL of distilled water was mixed with 1.76 g of CTAB and 3.20 mL of $NH_3{\cdot}H_2O$ for 30 min. 9.33 mL of TEOS was gradually added to the solution while being vigorously stirred, followed by an additional 2 h of stirring. The gel mixture was

https://doi.org/10.1021/acsomega.3c07214
ACS Omega 2023, 8, 43285−43294

aged at room temperature for 20 h. The resulting solid product was collected by filtering, thoroughly cleaned with 50% (v/v) ethanol aqueous solution to get rid of the remaining chemicals, and then dried at 80 °C for an extended period of time. Prior to use, the sample was calcined in air for 4 h at 550 °C.

4.3.2. Preparation of 12-HPW@MeSi. 0.667 g amount of 12-HPW was dissolved in 60 mL of distilled water followed by the addition of 2 g of the synthesized MeSi. The resulting mixture was vigorously stirred at room temperature for 22 h, followed by gradual evaporation of the solvent at 50 °C. It was dried at 100 °C overnight and then calcined at 300 °C for 2 h.

4.4. Transformation of Ginsenoside Rb1 with Ethanol. 2.0 mg of the ginsenoside Rb1 authentic standard and 44.3 mg of synthesized 12-HPW@MeSi were properly weighed and dissolved in 2.0 mL of 30% ethanol aqueous solution. The solution was cooled to room temperature after 4 h of heating at 80 °C in a shaking water bath. After centrifugation at 3000 rpm for 2 min, 200 μL of the clear reaction solution was collected and diluted to 1.0 mL, and the reaction solution was filtered through a 0.22 μm filter before HPL-MS analysis. The precipitate was collected and washed with a 50% (v/v) methanol aqueous solution. The resultant solid was then dried in a vacuum at 50 °C and used again for the transformation of Rb1.

■ ASSOCIATED CONTENT

Supporting Information

The Supporting Information is available free of charge at https://pubs.acs.org/doi/10.1021/acsomega.3c07214.

Fragmentation pathways and MS^2 spectrum of the $[M - H]^-$ ion at m/z 829.53 from the ginsenoside 20(R)-OC_2H_5-25-OH-Rg3 (Figure S1); fragmentation pathways and MS^2 spectrum of the $[M - H]^-$ ion at m/z 829.53 of ginsenoside 20(R)-25-OC_2H_5-Rg3 (Figure S2); fragmentation pathways and MS^2 spectrum of the $[M - H]^-$ ion at m/z 783.49 from the ginsenoside (20R, 25)-epoxy-Rg3 (Figure S3); fragmentation pathways and MS^2 spectrum of the $[M - H]^-$ ion at m/z 811.52 from the ginsenoside 25-OC_2H_5-Rk1 (Figure S4); fragmentation pathways and MS^2 spectrum of the $[M - H]^-$ ion at m/z 801.50 from the ginsenoside 20(S)-25-OH-Rg3 (Figure S5); fragmentation pathways and MS^2 spectrum of the $[M - H]^-$ ion at m/z 801.50 from the ginsenoside 20(R)-25-OH-Rg3 (Figure S6); fragmentation pathways and MS^2 spectrum of the $[M - H]^-$ ion at m/z 783.49 from the ginsenoside 25-OH-Rk1 (Figure S7); fragmentation pathways and MS^2 spectrum of the $[M - H]^-$ ion at m/z 783.49 from the ginsenoside 25-OH-Rg5 (Figure S8); fragmentation pathways and MS^2 spectrum of the $[M - H]^-$ ion at m/z 783.49 from the ginsenoside 20(S)-Rg3 (Figure S9); fragmentation pathways and MS^2 spectrum of the $[M - H]^-$ ion at m/z 783.49 from the ginsenoside 20(R)-Rg3 (Figure S10); fragmentation pathways and MS^2 spectrum of the $[M - H]^-$ ion at m/z 783.49 from the ginsenoside Rk1 (Figure S11); and fragmentation pathways and MS^2 spectrum of the $[M - H]^-$ ion at m/z 783.49 from the ginsenoside Rg5 (Figure S12) (PDF)

■ AUTHOR INFORMATION

Corresponding Authors

Huanxi Zhao − *Jilin Ginseng Academy, Changchun University of Chinese Medicine, Changchun 130117, P. R. China*; Email: phoenix8713@sina.com

Yang Xiu − *Jilin Ginseng Academy, Changchun University of Chinese Medicine, Changchun 130117, P. R. China*; orcid.org/0009-0003-4455-5331; Email: xiuyang@ccucm.edu.cn

Authors

Mengya Zhao − *Jilin Ginseng Academy, Changchun University of Chinese Medicine, Changchun 130117, P. R. China*

Lu Tian − *Jilin Ginseng Academy, Changchun University of Chinese Medicine, Changchun 130117, P. R. China*

Yusheng Xiao − *Jilin Ginseng Academy, Changchun University of Chinese Medicine, Changchun 130117, P. R. China*

Yanyan Chang − *Jilin Ginseng Academy, Changchun University of Chinese Medicine, Changchun 130117, P. R. China*

Yujiang Zhou − *Jilin Ginseng Academy, Changchun University of Chinese Medicine, Changchun 130117, P. R. China*

Shuying Liu − *Jilin Ginseng Academy, Changchun University of Chinese Medicine, Changchun 130117, P. R. China*

Complete contact information is available at: https://pubs.acs.org/10.1021/acsomega.3c07214

Notes

The authors declare no competing financial interest.

■ ACKNOWLEDGMENTS

This work was financially supported by the Science and Technology Development Plan Project of Jilin Province (nos. 20210204098YY and YDZJ202201ZYTS261).

■ REFERENCES

(1) Christensen, L. P. Ginsenosides chemistry, biosynthesis, analysis, and potential health effects. *Adv. Food Nutr. Res.* **2008**, *55*, 1−99.

(2) Attele, A. S.; Wu, J. A.; Yuan, C. S. Ginseng pharmacology: multiple constituents and multiple actions. *Biochem. Pharmacol.* **1999**, *58* (11), 1685−1693.

(3) Lu, J.-M.; Yao, Q.; Chen, C. Ginseng Compounds: An Update on their Molecular Mechanisms and Medical Applications. *Curr. Vasc. Pharmacol.* **2009**, *7* (3), 293−302.

(4) Angelova, N.; Kong, H.-W.; Van Der Heijden, R.; Yang, S.-Y.; Choi, Y. H.; Kim, H. K.; Wang, M.; Hankemeier, T.; Van Der Greef, J.; Xu, G.; Verpoorte, R. Recent methodology in the phytochemical analysis of ginseng. *Phytochem. Anal.* **2008**, *19* (1), 2−16.

(5) Zhu, G.-Y.; Li, Y.-W.; Hau, D. K.-P.; Jiang, Z.-H.; Yu, Z.-L.; Fong, W.-F. Protopanaxatriol-Type Ginsenosides from the Root of Panax ginseng. *J. Agric. Food Chem.* **2011**, *59* (1), 200−205.

(6) Shin, K.-C.; Oh, D.-K. Characterization of a novel recombinant beta-glucosidase from Sphingopyxis alaskensis that specifically hydrolyzes the outer glucose at the C-3 position in protopanaxadiol-type ginsenosides. *J. Biotechnol.* **2014**, *172*, 30−37.

(7) Li, W.; Gu, C.; Zhang, H.; Awang, D. V.; Fitzloff, J. F.; Fong, H. H.; van Breemen, R. B. Use of high-performance liquid chromatography-tandem mass spectrometry to distinguish Panax ginseng C. A. Meyer (Asian ginseng) and Panax quinquefolius L. (North American ginseng). *Anal. Chem.* **2000**, *72* (21), 5417−5422.

(8) Nag, S. A.; Qin, J.-J.; Wang, W.; Wang, M.-H.; Wang, H.; Zhang, R. Ginsenosides as anticancer agents: in vitro and in vivo activities, structure-activity relationships, and molecular mechanisms of action. *Front. Pharmacol.* **2012**, *3*, 25.

(9) Huq, M. A.; Kim, Y.-J.; Min, J.-W.; Bae, K. S.; Yang, D.-C. Use of Lactobacillus rossiae DC05 for bioconversion of the major ginsenosides Rb1 and Re into the pharmacologically active ginsenosides C-K and Rg2. *Food Sci. Biotechnol.* **2014**, *23* (5), 1561−1567.
(10) Cui, L.; Wu, S.-q.; Zhao, C.-a.; Yin, C.-r. Microbial conversion of major ginsenosides in ginseng total saponins by Platycodon grandiflorum endophytes. *J. Ginseng Res.* **2016**, *40* (4), 366−374.
(11) Han, B. H.; Park, M. H.; Han, Y. N.; Woo, L. K.; Sankawa, U.; Yahara, S.; Tanaka, O. Degradation of ginseng saponins under mild acidic conditions. *Planta Med.* **1982**, *44* (3), 146−149.
(12) Bae, E. A.; Han, M. J.; Kim, E. J.; Kim, D. H. Transformation of ginseng saponins to ginsenoside Rh-2 by acids and human intestinal bacteria and biological activities of their transformants. *Arch. Pharmacal Res.* **2004**, *27* (1), 61−67.
(13) Heravi, M. M.; Fard, M. V.; Faghihi, Z. Heteropoly acids-catalyzed organic reactions in water: doubly green reactions. *Green Chem. Lett. Rev.* **2013**, *6* (4), 282−300.
(14) Coronel, N. C.; da Silva, M. J. Lacunar Keggin Heteropolyacid Salts: Soluble, Solid and Solid-Supported Catalysts. *J. Cluster Sci.* **2018**, *29* (2), 195−205.
(15) Omwoma, S.; Gore, C. T.; Ji, Y.; Hu, C.; Song, Y.-F. Environmentally benign polyoxometalate materials. *Coord. Chem. Rev.* **2015**, *286*, 17−29.
(16) Marcì, G.; Garcia-Lopez, E. I.; Palmisano, L. Heteropolyacid-Based Materials as Heterogeneous Photocatalysts. *Eur. J. Inorg. Chem.* **2014**, *2014* (1), 21−35.
(17) García-López, E. I.; Marci, G.; Pomilla, F. R.; Kirpsza, A.; Micek-Ilnicka, A.; Palmisano, L. Supported H3PW12O40 for 2-propanol (photo-assisted) catalytic dehydration in gas-solid regime: The role of the support and of the pseudo-liquid phase in the (photo)activity. *Appl. Catal., B* **2016**, *189*, 252−265.
(18) Chen, L.; Nohair, B.; Zhao, D.; Kaliaguine, S. Glycerol acetalization with formaldehyde using heteropolyacid salts supported on mesostructured silica. *Appl. Catal., A* **2018**, *549*, 207−215.
(19) Narkhede, N.; Singh, S.; Patel, A. Recent progress on supported polyoxometalates for biodiesel synthesis via esterification and transesterification. *Green Chem.* **2015**, *17* (1), 89−107.
(20) Ren, Y.; Yue, B.; Gu, M.; He, H. Progress of the Application of Mesoporous Silica-Supported Heteropolyacids in Heterogeneous Catalysis and Preparation of Nanostructured Metal Oxides. *Materials* **2010**, *3* (2), 764−785.
(21) Heravi, M. M.; Sadjadi, S. Recent Developments in Use of Heteropolyacids, Their Salts and Polyoxometalates in Organic Synthesis. *J. Iran. Chem. Soc.* **2009**, *6* (1), 1−54.
(22) Kim, H.-J.; Shul, Y.-G.; Han, H. Sulfonic-functionalized heteropolyacid-silica nanoparticles for high temperature operation of a direct methanol fuel cell. *J. Power Sources* **2006**, *158* (1), 137−142.
(23) Yang, Y.; Lv, G.; Guo, W.; Zhang, L. Synthesis of mesoporous silica-included heteropolyacids materials and the utilization for the alkylation of phenol with cyclohexene. *Microporous Mesoporous Mater.* **2018**, *261*, 214−219.
(24) Fu, Y.; Yin, Z. H.; Yin, C. Y. Biotransformation of ginsenoside Rb1 to ginsenoside Rg3 by endophytic bacterium Burkholderia sp GE 17-7 isolated from Panax ginseng. *J. Appl. Microbiol.* **2017**, *122* (6), 1579−1585.
(25) Bai, Y.; Gaenzle, M. G. Conversion of ginsenosides by *Lactobacillus plantarum* studied by liquid chromatography coupled to quadrupole trap mass spectrometry. *Food Res. Int.* **2015**, *76*, 709−718.
(26) Xiu, Y.; Zhao, H.; Gao, Y.; Liu, W.; Liu, S. Chemical transformation of ginsenoside Re by a heteropoly acid investigated using HPLC-MSn/HRMS. *New J. Chem.* **2016**, *40* (11), 9073−9080.
(27) Cao, J.; Liu, C.; Wang, Q. Q.; Li, Y. Z.; Yu, Q. A novel catalytic application of heteropolyacids: chemical transformation of major ginsenosides into rare ginsenosides exemplified by R-g1. *Sci. China: Chem.* **2017**, *60* (6), 748−753.
(28) Lee, S. M.; Seo, H. K.; Oh, J.; Na, M. Updating chemical profiling of red ginseng via the elucidation of two geometric isomers of ginsenosides Rg9 and Rg10. *Food Chem.* **2013**, *141* (4), 3920−3924.
(29) Perez de Souza, L.; Alseekh, S.; Scossa, F.; Fernie, A. R. Ultra-high-performance liquid chromatography high-resolution mass spectrometry variants for metabolomics research. *Nat. Methods* **2021**, *18* (7), 733−746.
(30) Vaniya, A.; Fiehn, O. Using fragmentation trees and mass spectral trees for identifying unknown compounds in metabolomics. *TrAC, Trends Anal. Chem.* **2015**, *69*, 52−61.
(31) Jeong, S. M.; Lee, J. H.; Kim, J. H.; Lee, B. H.; Yoon, I. S.; Lee, J. H.; Kim, D. H.; Rhim, H.; Kim, Y.; Nah, S. Y. Stereospecificity of ginsenoside Rg(3) action on ion channels. *Mol. Cells* **2004**, *18* (3), 383−389.
(32) Yu, H.; Wang, Y.; Liu, C.; Yang, J.; Xu, L.; Li, G.; Song, J.; Jin, F. Conversion of Ginsenoside Rb1 into Six Types of Highly Bioactive Ginsenoside Rg3 and Its Derivatives by FeCl3 Catalysis. *Chem. Pharm. Bull.* **2018**, *66* (9), 901−906.
(33) Li, D.; Liao, M. Study on the dehydrofluorination of vinylidene fluoride (VDF) and hexafluoropropylene (HFP) copolymer. *Polym. Degrad. Stab.* **2018**, *152*, 116−125.
(34) Chen, L.; Zhang, L.; Yan, G.; Huang, D. Recent Advances of Cinnamic Acids in Organic Synthesis. *Asian J. Org. Chem.* **2020**, *9* (6), 842−862.

https://doi.org/10.1021/acsomega.3c07214
ACS Omega 2023, 8, 43285−43294